In vivo volumetric imaging of chicken retina with ultrahigh-resolution spectral domain optical coherence tomography

Alireza Akhlagh Moayed,[1] Sepideh Hariri,[1] Eun Sun Song,[1] Vivian Choh,[2] and Kostadinka Bizheva[1,*]

[1]*Department of Physics and Astronomy, University of Waterloo, Waterloo, ON N2L3G1, Canada*
[2]*School of Optometry, University of Waterloo, Waterloo, ON N2L3G1, Canada*
**kbizheva@uwaterloo.ca*

Abstract: The chicken retina is an established animal model for myopia and light-associated growth studies. It has a unique morphology: it is afoveate and avascular; oxygen and nutrition to the inner retina is delivered by a vascular tissue (pecten) that protrudes into the vitreous. Here we present, to the best of our knowledge, the first *in vivo*, volumetric high-resolution images of the chicken retina. Images were acquired with an ultrahigh-resolution optical coherence tomography (UHROCT) system with 3.5 μm axial resolution in the retina, at the rate of 47,000 A-scans/s. Spatial variations in the thickness of the nerve fiber and ganglion cell layers were mapped by segmenting and measuring the layer thickness with a semi-automatic segmentation algorithm. Volumetric visualization of the morphology and morphometric analysis of the chicken retina could aid significantly studies with chicken retinal models of ophthalmic diseases.

OCIS codes: (170.4500) Optical coherence tomography; (170.3880) Medical and Biological Imaging; (100.2960) Image analysis; (170.4470) Ophthalmology

References and links

1. J. Wallman, J. Turkel, and J. Trachtman, "Extreme myopia produced by modest change in early visual experience," Science **201**(4362), 1249–1251 (1978).
2. E. L. Irving, M. G. Callender, and J. G. Sivak, "Inducing myopia, hyperopia, and astigmatism in chicks," Optom. Vis. Sci. **68**(5), 364–368 (1991).
3. C. F. Wildsoet and J. Wallman, "Choroidal and scleral mechanisms of compensation for spectacle lenses in chicks," Vision Res. **35**(9), 1175–1194 (1995).
4. V. B. Morris, "An afoveate area centralis in the chick retina," J. Comp. Neurol. **210**(2), 198–203 (1982).
5. Y. Zhang, J. Xu, M. Garcia, A. Roorda, and C. Wildsoet, "In vivo imaging the photoreceptors in the chicken eye with adaptive optics scanning laser ophthalmoscope," J. Vis. **9**(14), 79–000 (2009).
6. K. Headington, S. S. Choi, D. Nickla, and N. Doble, "Single cell, in-vivo imaging of chick retina with adaptive optics," Invest. Ophthalmol. Vis. Sci. **51**, Abstract 2321 (2010).
7. M. L. Kisilak, J. J. Hunter, E. L. Irving, and M. C. W. Campbell, "In vivo imaging of photoreceptors in the alert chicken," Invest. Ophthalmol. Vis. Sci. **48**, Abstract 1191 (2007).
8. D. Huang, E. A. Swanson, C. P. Lin, J. S. Schuman, W. G. Stinson, W. Chang, M. R. Hee, T. Flotte, K. Gregory, C. A. Puliafito, and J. G. Fujimoto, "Optical coherence tomography," Science **254**(5035), 1178–1181 (1991).
9. A. F. Fercher, "Optical coherence tomography," J. Biomed. Opt. **1**(2), 157–000 (1996).
10. Y. Huang, A. V. Cideciyan, G. I. Papastergiou, E. Banin, S. L. Semple-Rowland, A. H. Milam, and S. G. Jacobson, "Relation of optical coherence tomography to microanatomy in normal and rd chickens," Invest. Ophthalmol. Vis. Sci. **39**(12), 2405–2416 (1998).
11. M. Ruggeri, J. C. Major, Jr., C. McKeown, R. W. Knighton, C. A. Puliafito, and S. Jiao, "Retinal structure of birds of prey revealed by ultra-high resolution spectral-domain optical coherence tomography," Invest. Ophthalmol. Vis. Sci. **51**(11), 5789–5795 (2010).
12. P. Puvanathasan, P. Forbes, Z. Ren, D. Malchow, S. Boyd, and K. Bizheva, "High-speed, high-resolution Fourier-domain optical coherence tomography system for retinal imaging in the 1060 nm wavelength region," Opt. Lett. **33**(21), 2479–2481 (2008).
13. S. Hariri, A. A. Moayed, A. Dracopoulos, C. Hyun, S. Boyd, and K. Bizheva, "Limiting factors to the OCT axial resolution for in-vivo imaging of human and rodent retina in the 1060 nm wavelength range," Opt. Express **17**(26), 24304–24316 (2009).

#143543 - $15.00 USD Received 3 Mar 2011; revised 2 Apr 2011; accepted 15 Apr 2011; published 19 Apr 2011

14. E. L. Irving, J. G. Sivak, T. A. Curry, and M. G. Callender, "Chick eye optics: zero to fourteen days," J. Comp. Physiol. A Neuroethol. Sens. Neural Behav. Physiol. **179**(2), 185–194 (1996).
15. M. Wojtkowski, V. J. Srinivasan, T. H. Ko, J. G. Fujimoto, A. Kowalczyk, and J. S. Duker, "Ultrahigh-resolution, high-speed, Fourier domain optical coherence tomography and methods for dispersion compensation," Opt. Express **12**(11), 2404–2422 (2004).
16. A. Mishra, A. Wong, K. Bizheva, and D. A. Clausi, "Intra-retinal layer segmentation in optical coherence tomography images," Opt. Express **17**(26), 23719–23728 (2009).
17. I. G. Morgan, "Intraocular colchicine selectively destroys immature ganglion cells in chicken retina," Neurosci. Lett. **24**(3), 255–260 (1981).
18. V. Choh, J. Banh, and C. F. Wildsoet, "Thickness and histological changes in optic nerve-sectioned chick retina," Invest. Ophthalmol. Vis. Sci. **45**, E-Abstract 47 (2004).

1. Introduction

The chicken is a widely used animal for studies of ocular development and eye growth. It has been, and continues to be, the first model used in studies examining the factors and mechanisms mediating refractive error development [1–3]. Chickens are diurnal, and their retinas contain cones and rods, however, the chicken eye has several structures or adaptations that differ from their mammalian counterparts. For example, chickens are afoveate, having instead, an area centralis [4] and their retinas are devoid of blood vessels; the pecten, a sheet of vascular tissue that protrudes into the vitreous chamber, supplies the internal milieu of the eye with oxygen and nutrients. Recently, *in vivo* images of photoreceptors in the chicken retina with adaptive optics laser scanning ophthalmoscope (AO-SLO) were reported [5–7], suggesting that optical imaging techniques could prove an excellent research tool for longitudinal studies of chicken models of ophthalmic diseases. Although the AO-SLO technique offers high lateral resolution in the living retina, the axial imaging resolution is limited by the optics of the eye and the imaging wavelength, and thus precise volumetric imaging of retinal morphology is not feasible.

Optical coherence tomography (OCT) is a non-invasive imaging modality based on detection of partially coherent light, that can provide depth-resolved, cellular level resolution imaging of the structural composition of biological tissue at depths of 1-2 mm below the surface [8,9]. Pioneer cross-sectional images of healthy chicken retina were first acquired with a slow scanning, Time-Domain OCT system [10]. However, significant development in OCT technology over the past decade has led to ~10x improvement in the OCT axial resolution and more than 100x improvement in the OCT image acquisition rate. While *in vivo* ultrahigh-resolution OCT (UHROCT) images of the avian retina in birds of prey were recently reported [11], birds of prey have a different retinal morphology compared to the various species of chicken that are typically used in studies of myopia or retinal degeneration.

Here we present preliminary results from a morphometric study of the healthy chicken retina, conducted with a research grade UHROCT system. Volumetric images of a healthy chicken retina were acquired *in vivo* and a custom segmentation algorithm was used to measure spatial variations of the individual retinal layers. As a first step in assessing UHROCT as a modality for imaging chicken retinal morphology, UHROCT images and traditional histological micrographs of the same retina were compared.

2. Methods

2.1. Imaging system description

A high speed, spectral domain UHROCT system operating at ~1060 nm was used for *in vivo* imaging of the chicken retina. Details about the imaging system design and performance for *in vivo* imaging of the human and rat were published previously [12,13]. Briefly, the UHROCT system is based on a spectral domain design. The system core is a fiberoptic Michelson-Morley interferometer, interfaced to a broad bandwidth superluminescent diode (SLD)-based light source (Superlum Ltd., λc = 1020 nm, $\Delta\lambda$ = 110 nm, P_{out} = 10 mW). The SLD spectral output was a custom shaped to provide higher power at ~980nm, where water absorption has a local maximum. Considering the average axial length of 13 day old chicken eye (~8mm [14]) the spectral shaping resulted in 3.5 µm UHROCT axial resolution in the chicken retina. An

#143543 - $15.00 USD Received 3 Mar 2011; revised 2 Apr 2011; accepted 15 Apr 2011; published 19 Apr 2011

imaging probe composed of an achromat doublet collimator (Edmund Optics, f = 12 mm), a pair of galvanometric scanners (Cambridge Technologies) and a pair of achromat doublet lenses (Edmund Optics, f = 60 mm and f = 30 mm) was designed and built for imaging of the chicken retina. The diameter of the imaging beam was ~1.25 mm at the cornea, resulting in lateral imaging resolution in the chicken retina of about 5 µm. The OCT lateral resolution at the chicken retina surface was estimated by creating a ZEMAX model of the OCT imaging probe and the chicken eye and considering both the monochromatic and polychromatic aberrations. Information about the refractive indexes, thickness and curvature of the chicken eye cornea, lens and vitreous were obtained from the available literature [14]. The OCT interference signal was detected with a custom, high performance spectrometer (P&P Optica Inc.), interfaced to a 1024 pixel linear array InGaAs camera (SUI, Goodrich Corp.) with a data transfer rate of 47 kHz. The UHROCT system provided ~99 dB SNR for 1.7 mW power of the imaging beam. Dispersion within the imaging system, due to the optical and fiberoptic components, was compensated for by the use of a tunable dispersion compensation unit composed of a pair of BK7 prisms (Edmund Optics), connected to each other with an optical gel (Thorlabs) and attached to a pair of miniature manual translation stages (Edmund Optics). Dispersion arising from the optics of the chicken eye was compensated for numerically with an algorithm based on a previously published method [15]. The OCT image acquisition code is based on LabView (National Instruments). Retinal 2D tomograms were generated from the raw data and processed with Matlab (Mathworks). The imaging data was rendered in 3D using Amira software (Visage Imaging Inc.). A semi-automatic segmentation algorithm, developed in our research group [16] was used for segmentation and thickness measurement of selected retinal layers.

2.2. Animals

A 13 days old White Leghorn (Gallus gallus domesticus) chicken was used in the study. The imaging procedure was approved by the University of Waterloo Animal Ethics Committee. The chicken was anesthetized with 1% isoflurane and placed on a custom-designed holder that keeps the animal stationary during the imaging session and allows for easy alignment of the eye with respect to the imaging probe. The imaging procedure was carried out in semi-dark environment to achieve natural pupil dilation and pupil diameter was measured to be larger than 2.5 mm throughout the entire imaging procedure. Constant pupil size was confirmed by the absence of obstructions and vignetting that would have occurred had the imaging beam been larger. A retractor was used to keep the eyelid open during the imaging procedure and artificial tear drops were administered frequently to keep the cornea well hydrated and transparent.

2.3. Histology

Following the UHROCT imaging session, the chicken was decapitated and the eyes were immediately enucleated. Incisions were made at the ora serrata and the anterior segment and vitreous were removed. The remaining eyecup was fixed in freshly prepared 4% (w/v) para-formaldehyde with 3% (w/v) sucrose in 0.1 M Sorensen's buffer (pH 7.5; SB) for 20 min. Eyecups were then rinsed in 0.1 M SB (3 x 10 minutes) before being cryoprotected (30% (w/v) sucrose in SB, overnight). The next day, the eyes were embedded in Optimal Cutting Temperature embedding medium and then were frozen, before being sectioned in a cryostat onto clean glass slides. Sections were 12 µm or 18 µm thick and were allowed to air-dry prior to staining with hemotoxylin and eosin (H & E). Coverslips were mounted onto the slides using Permount and images of the sections were captured with a light microscope and color camera (Carl Zeiss).

3. Results and Discussion

Multiple 3D image stacks with dimensions 1000 × 512 × 256 (A-scans x Pixels x B-scans) were acquired from the chicken retina at wide (~20°) and narrow (~7°) scanning angles. Figure 1 shows representative UHROCT images of the chicken retina at locations away from

#143543 - $15.00 USD Received 3 Mar 2011; revised 2 Apr 2011; accepted 15 Apr 2011; published 19 Apr 2011

(A) and near the optical nerve head (C), and corresponding H&E stained histological cross-sections of the same regions (Fig. 1B and 1D, respectively). Scale bars provided in all images allow for determination of the size and spatial separation of morphological features in the chicken retina. All retinal layers are clearly visualized in the UHROCT tomograms and match well with the retinal layers as observed in the histological cross-sections (Fig. 1B, and 1D). The ganglion cell layer (GCL) is clearly visible in the UHROCT images as a bright band located immediately below the dark, highly scattering nerve finer layer (NFL). The NFL thickness varies with location in the retina and is thickest at the optic nerve head (ONH). The chicken retina has a fairly thin outer nuclear layer compared to mammalian retinas, which is clear from the images in Fig. 1. The external limiting membrane appears on the UHROCT tomograms as a very distinct dark gray line above the low scattering photoreceptor layer.

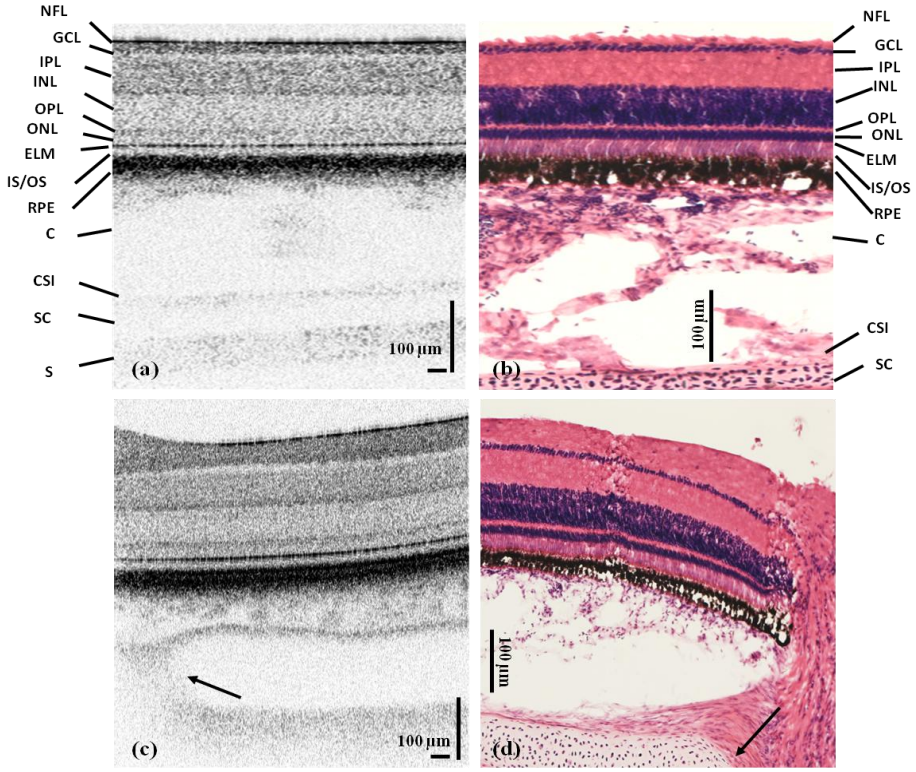

Fig. 1. Representative UHROCT tomograms of the chicken retina acquired from locations away (A) and near (C) the ONH, compared with H&E stained histology (B and D). Individual retinal layers observed in the UHROCT tomograms match well with corresponding layers in the histological cross-sections. The black arrows in C and D mark the termination of the cartilaginous sclera layer near the optical nerve head.

The chorio-scleral interface (CSI) is clearly visible on both UHROCT images. The chicken sclera contains a fairly thick cartilaginous layer (SC), separating the choroid from the fibrous sclera (S). The cartilaginous sclera is composed of cells with a large cytoplasm to nucleus ratio, thus rendering the cartilage almost transparent to infrared light. Termination of the cartilage is clearly observed near the ONH (Fig. 1C and 1D, black arrows). The apparent difference in the choroidal thickness observed between the UHROCT and histological cross-sections is most likely a post-mortem artifact due to the choroid moving away from the retina during the cryo-sectioning.

Figure 2 shows rendered volumetric stacks from different locations in the chicken retina acquired at wide (A, B and C) and narrow (D) scanning angles. These volumes are comprised

#143543 - $15.00 USD Received 3 Mar 2011; revised 2 Apr 2011; accepted 15 Apr 2011; published 19 Apr 2011

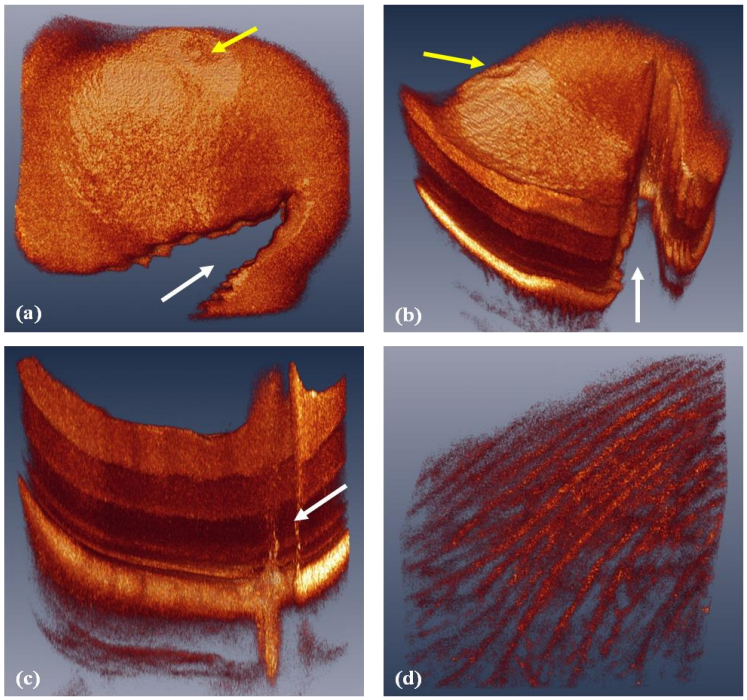

Fig. 2. Selected frames from rendered volumetric image stacks of the chicken retina acquired at wide (A, B and C) and narrow (D) scanning angles. Different views of the pecten layer are presented in A (Media 1), B and C (Media 2) and marked with white arrows. An area in the retina with significantly thinner NFL is marked with yellow arrows in A and B. A view of the choroidal vasculature is shown in D (Media 3).

of 256 B-scans (1000 x 512), corresponding to ~3 mm x 3 mm (wide angle) and ~1mm x 1 mm (narrow scanning angle) area on the tissue surface. The volumetric images presented in Fig. 2A, 2B and 2C, were acquired from a location in the retina close to the pecten (white arrows). Since the pecten is a highly vascular tissue, light absorption and scattering within the blood vessel in the pecten produces a shadowing effect in the UHROCT tomograms. The folds of the pecten can be observed clearly on the *en face* (Fig. 3A and 3B) and cross-sectional movies (Fig. 2C). The volumetric images in Fig. 2A and 2B also show an area at the retinal surface with significantly thinner NFL. This area, located about 2 mm away from the ONH, appears darker, more transparent and round in shape (Fig. 2A and 2B, yellow arrows), and is tentatively speculated to represent the area centralis of the chicken retina. Further examination of other retinal layers in this area is required for confirmation of this hypothesis. The movie frame in Fig. 2D shows a view of the chicken retina choroidal vasculature.

Figure 3 shows representative B-scans that were used to generate the volumetric image presented in Fig. 2A. The image in Fig. 3A shows a cross-sectional view of the pecten (black arrow). This image also shows thickening of the NFL, thinning of the choroid and termination of the sclera cartilage near the ONH. The images shown in Fig. 3B, 3C and 3D show progressive thinning of the NFL and thickening of both the GCL and the choroid in one location in the retina.

Morphometric analysis of the chicken retina could be very helpful in various chicken models of retinal diseases. Here we used a semi-automatic segmentation algorithm developed segmented NFL and GCL is shown in Fig. 4C (red lines). *En face* thickness maps of the NFL and the GCL are shown in Fig. 4B and 4D, respectively. A Gaussian blur algorithm (10 pixels) was used to smooth the jagged appearance of the thickness maps, which is related to the axial OCT resolution and the limited number of B-scans (256) in the 3D imaging stack of

#143543 - $15.00 USD Received 3 Mar 2011; revised 2 Apr 2011; accepted 15 Apr 2011; published 19 Apr 2011

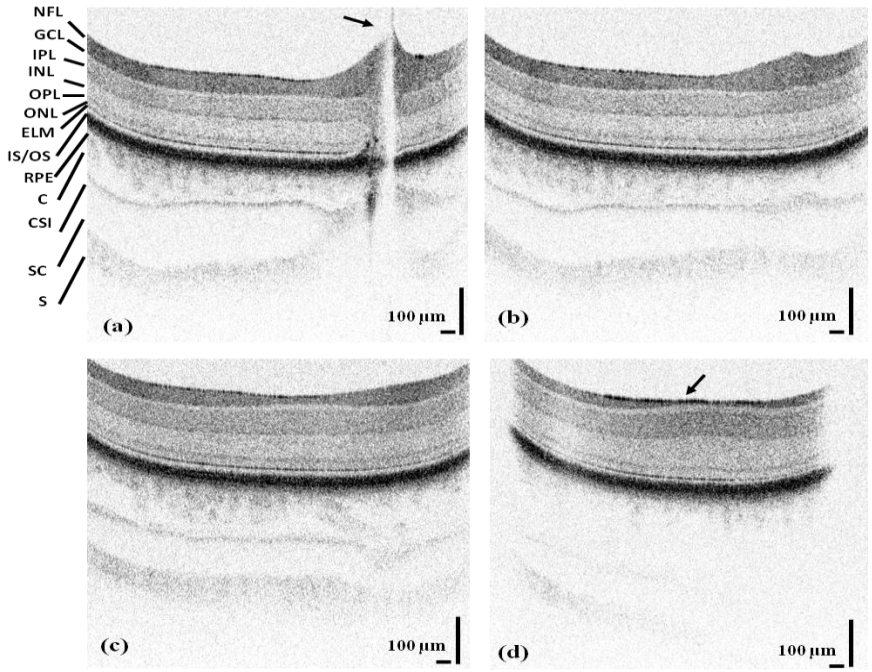

Fig. 3. Selected B-scans from the volumetric data set presented in Fig. 2A. Thickening of the NFL, thinning of the choroid and termination of the sclera cartilage are observed close to the pecten in the vicinity of the ONH (A). Progressive thinning of the NFL and thickening of the GCL and the choroid at a certain area in the retina are shown in B, C and D (black arrow). Image dimensions are 1000 x 512 (A-scans x pixels).

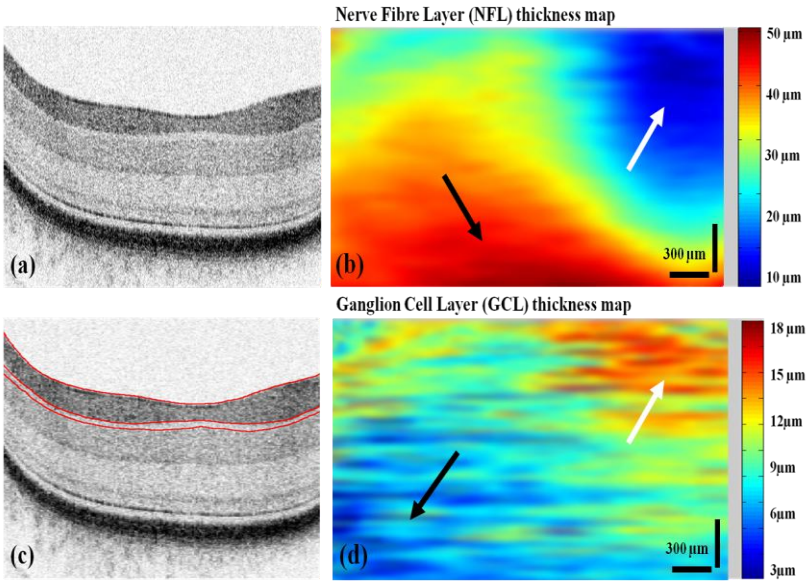

Fig. 4. Original UHROCT cross-section of the chicken retina (A); the same image with segmented NFL and GCL (C, red lines); thickness maps of the NFL (B) and the GCL (D). Black arrows mark locations close to the pecten and the ONH, while white arrows mark a location with significantly thinner NFL.

#143543 - $15.00 USD Received 3 Mar 2011; revised 2 Apr 2011; accepted 15 Apr 2011; published 19 Apr 2011

the retina, covering a square area of ~3 mm x 3 mm. In the NFL thickness map (Fig. 4B), the area closer to the ONH and the pecten is significantly (~50 µm) thicker (black arrow), while an area located ~2 mm away has a thickness of ~10 µm to 15 µm (white arrow). Similar areas at approximately the same locations are observed in the GCL thickness map (Fig. 4D). In this case, the area near the ONH and the pecten has a non-existent GCL, while the area marked with the white arrow has a GCL of ~15 µm average thickness. No significant spatial variation in the thickness of the remaining retinal layers was observed in the healthy chicken imaged in this study. It is expected that such thickness changes can occur in some retinal degenerative diseases, which will be the focus of future studies.

4. Conclusions

A research grade UHROCT system was used to acquire *in vivo* volumetric images of the healthy chicken retina and to quantify the spatial variation of the thickness of individual retinal layers. The UHROCT cross-sectional images showed excellent comparison with histological images. The volumetric UHROCT tomograms revealed quantifiable thickness changes to the various retina layers depending on location, including a region in which the nerve fiber layer was thinner, and the ganglion cell layer, thicker, than the surrounding area. Confirmation that this area is equivalent to the area centralis is necessary and if proven true, would give us an opportunity to add to the limited data sets that currently exist for this area.

Acknowledgments

This work was supported in part by research grants from the Natural Sciences and Engineering Research Council of Canada (NSERC) and the Canadian Foundation for Innovation (CFI). The authors would like to thank A. Zam for assistance with the ZEMAX model of the chicken eye and the imaging probe, and M. Campbell for the helpful discussions regarding the chicken eye.

#143543 - $15.00 USD Received 3 Mar 2011; revised 2 Apr 2011; accepted 15 Apr 2011; published 19 Apr 2011